Journal of Crystal Growth 311 (2009) 299–303

Contents lists available at ScienceDirect

Journal of Crystal Growth

journal homepage: www.elsevier.com/locate/jcrysgro

Effects of CeO_2 buffer layer thickness on the orientation and dielectric properties of $Ba(Zr_{0.20}Ti_{0.80})O_3$ thin films

Lina Gao, Jiwei Zhai *, Sangnian Song, Xihong Hao, Xi Yao

Functional Materials Research Laboratory, Tongji University, 1239 Siping Road, Shanghai 200092, China

ARTICLE INFO

Article history:
Received 22 July 2008
Received in revised form
17 November 2008
Accepted 17 November 2008
Communicated by D.P. Norton
Available online 21 November 2008

PACS:
77.22.Ch
77.55.+f
77.80.Bh

Keywords:
A1. Crystal structure
A1. X-ray diffraction
B1. Oxides
B2. Ferroelectric materials

ABSTRACT

$Ba(Zr_{0.20}Ti_{0.80})O_3$ (BZT) thin films are deposited on Pt(111)/Ti/SiO_2/Si(100) substrates by the sol–gel technique. The thickness of the CeO_2, serving as a buffer layer, is varied from 0 to 20 nm, to study the dependence of the orientation and dielectric properties of the BZT thin films on the buffer layer thickness. The influence of buffer layer thickness on the microstructure of the thin films is also examined. Dielectric properties of the thin films are investigated as a function of temperature and direct current electric field. The results show that the CeO_2 buffer layer strongly influences the orientation, microstructure and the dielectric properties of the films. The BZT thin films with 5 nm thickness CeO_2 buffer layer have the least loss, smallest leakage current and largest figure of merit (FOM).

1. Introduction

In recent years, great attention has been paid to electric field tunable dielectric materials due to their potential applications in tunable microwave devices, such as frequency-agile filters, voltage-controlled oscillators, phase shifters, and antennas. Among them, the environment friendly lead-free perovskite-structured barium strontium titanate (Ba, Sr)TiO_3 (BST) solid solution is mostly studied because of its relatively low dielectric loss, high dielectric constant, and large electric-field-dependent tunability [1–3]. $Ba(Zr_xTi_{1-x})O_3$ (BZT) is a possible alternative to BST in the fabrication of ceramic capacitors because Zr^{4+} is chemically more stable than Ti^{4+} [4–6]. The nature of the ferroelectric phase transition at Curie temperature (T_C) of BZT bulk ceramics is known to change strongly with the Zr content. At higher Zr contents ($x\sim0.20$), only one phase transition exists [7]. Furthermore, $Ba(Zr_xTi_{1-x})O_3$ ferroelectric in the paraelectric state reveals relatively more outstanding temperature stability compared with $(Ba_{1-x}Sr_x)TiO_3$ [6,8]. The dielectric constant of BZT can also be controlled electrically by applying a direct current (DC) electric field bias across it. Field-dependent dielectric constant of BZT may be exploited for radio frequency (RF) and microwave tunable filter applications [9,10].

Many efforts have been made to improve the dielectric properties of the BZT thin film capacitors, including using conductive oxide electrodes such as $LaNiO_3$ [11], $La_{0.7}Ca_{0.3}MnO_3$ [6], and $CaRuO_3$ [12]; changing the orientation of the BZT films [13] and adding dopants [14]. Our previous research [13] has shown that the orientation and dielectric properties of BZT thin films prepared by sol–gel process can be tailored by introducing the CeO_2 buffer layers. In this work, we present the results of dielectric properties of $Ba(Zr_{0.20}Ti_{0.80})O_3$ (BZT) thin films deposited on Pt(111)/Ti/SiO_2/Si(100) substrates, using CeO_2 buffer layers with varying thicknesses. The influences of buffer layer thickness and stress on the phase structure, microstructure, orientation, and dielectric properties of the BZT thin films are examined. The possible reason resulting in the change of ferroelectric behavior is discussed.

2. Experimental procedure

Barium acetate [$Ba(CH_3COO)_2$], zirconium (IV) isopropoxide [$Zr(OC_3H_7)_4$], and terabutyl titanate [$Ti(OC_4H_9)_4$] are used as starting materials. Glacial acetate acid is used as a solvent.

---

*Corresponding author. Tel.: +86 21 65980544; fax: +86 21 65985179.
E-mail address: apzhai@mail.tongji.edu.cn (J. Zhai).

0022-0248/$ - see front matter © 2008 Elsevier B.V. All rights reserved.
doi:10.1016/j.jcrysgro.2008.11.062

The barium acetate is initially dissolved in heated acetate acid according to the predetermined ratios. After cooling to room temperature, $Zr(OC_3H_7)_4$ and $Ti(OC_4H_9)_4$ are added in above solution. The ethyleneglycol monoethyl ether and acetylacetone are added to control the viscosity and cracking of films and the solution is mixed and refluxed for 1 h. The concentration of the final solution is adjusted to about 0.05 M. For the preparation of CeO_2 solution, the magnesium nitrate hexahydrate $[Ce(NO_3)_4 6H_2O]$ is used as starting materials and acetylacetone is used as a solvent. The CeO_2 buffer layers are prepared by spin coating on the Pt(111)/Ti/SiO_2/Si(100) substrates at 3000 rpm for 20 s each layer. Each spin-coated CeO_2 layer is subsequently heat treated in air at 700 °C on a hot plate for 5 min. The thickness of CeO_2 buffer layers are 5, 10, 15, and 20 nm in this study.

The BZT layers are deposited on the Pt(111)/Ti/SiO_2/Si(100) and CeO_2-buffered Pt(111)/Ti/SiO_2/Si(100) substrates, using the same coating process. After each coating, the films are heat treated in air at 700 °C on a hot plate for 5 min. The coating and heat treatment procedures are repeated until the desired thickness is reached. BZT films with a thickness of 350 nm are grown in this study.

The crystalline phase of the thin films is identified by X-ray diffraction (BRUKER D8 Advance diffractometer). F20 filmetrics is employed to measure the thickness of the films. The surface morphology is determined by atomic force microscopy (SPA-300HV). Au top electrode having a diameter 0.5 mm is deposited on top of the BZT thin films by DC-sputtering in order to measure electrical properties. The current–voltage (I–V) characteristics are measured using a Keithley 6517 A. The capacitance–voltage (C–V) and capacitance–temperature (C–T) characteristics are measured using an Agilent 4284 A LCR meter.

3. Results and discussion

Fig. 1 shows the X-ray diffraction patterns of the BZT thin films with different CeO_2 buffer layer thicknesses. The diffraction peaks from the films can be indexed as perovskite BZT in the absence of other phases reflecting the phase compatibility between CeO_2 and BZT. The peak at 2θ of 28.5° appearing for c–e in Fig. 1 is indexed as the (111) CeO_2 reflection. For the films directly deposited on Pt(111)/Ti/SiO_2/Si(100) substrate, (111)-oriented structure with intense (111) peak is obtained. The relative peak intensity of $I(111)/\Sigma I(h\,k\,l)$ is found to be 0.582, indicating a preferential (111) orientation. The small mismatch between BZT (111) and Pt (111) is about 2.8%, which might lead to the preferential (111)-oriented BZT films on (111)-textured Pt bottom electrodes [15]. For the films deposited on CeO_2-buffered Pt(111)/Ti/SiO_2/Si (100) substrates, (110) preferred orientation is obtained. The relative peak intensities of $I(110)/\Sigma I(h\,k\,l)$ are found to be 0.564, 0.576, 0.590, and 0.606 for the BZT films with CeO_2 buffer layer thicknesses 5, 10, 15, and 20 nm, indicating preferential (110) orientation. This result suggests that CeO_2 is a viable template for highly (110)-oriented BZT film growth. Same result has been reported by other researchers [16]. The above results indicate that the CeO_2 buffer layers can affect the texture of BZT thin films on Pt(111)/Ti/SiO_2/Si(100) substrates.

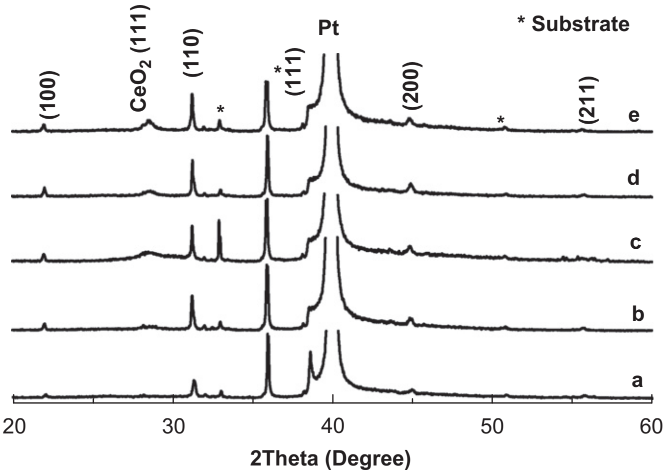

Fig. 1. XRD patterns of BZT thin films with different CeO_2 buffer layer thickness: (a) 0 nm, (b) 5 nm, (c) 10 nm, (d) 15 nm, and (e) 20 nm.

The average grain size and the surface roughness of the films are analyzed with AFM in tapping mode amplitude modulation. The AFM images are obtained by using an area of $1\,\mu m \times 1\,\mu m$. The surface AFM micrographs for the BZT thin films with different CeO_2 buffer layer thickness deposited on Pt substrates are shown in Fig. 2. All the AFM images show smooth surface morphology and the absence of both cracks and pinholes. It can also be clearly seen that the surface morphologies are strongly influenced by the CeO_2 buffer layer. As the thickness of CeO_2 buffer layer increases, the grain size of the BZT thin films decreases. The average roughness parameter (R_a) are 4.4, 3.9, 3.7, 3.4, and 3.1 nm for the BZT films with buffer layer thicknesse 0, 5, 10, 15, and 20 nm. This result suggests that the CeO_2 buffer layer substantially influences the crystallization behavior and the microstructure of BZT thin films. The average grain size of the BZT thin films with different CeO_2 buffer layer thickness is 30–45 nm.

Fig. 3 shows the temperature-dependent dielectric constant of BZT films with different CeO_2 buffer layer thickness measured in the frequency range 100–1000 kHz. The dielectric constant of BZT thin films is much lower than that of $Ba(Zr_{0.20}Ti_{0.80})O_3$ ceramics (ε_r=5900) reported by Chou et al. [17]. The broad nature of the plot indicates the diffuse phase transition from ferroelectric to paraelectric phase. The transition temperature, corresponding to the dielectric maxima, is −50 °C, which is lower than that of bulk $Ba(Zr_{0.20}Ti_{0.80})O_3$ ceramics ($T_C \approx 40\,^{\circ}C$) [17]. It is noteworthy that the Curie temperature moves to a higher temperature when the BZT thin films are deposited on CeO_2-buffered Pt(111)/Ti/SiO_2/Si(100) substrates. With the increase of CeO_2 buffer layer thickness from 0 to 20 nm, the Curie temperature increases from −50 to 60 °C. The upward shift of T_C in the BZT thin films is believed to be due to the stress inside the films. In chemical solution-derived films, there is a significant decease in film volume during evaporation, pyrolysis, and densification. Biaxial tensile stresses arise within the film because the volume change is constrained by the substrate. These tensile stresses can be relieved by increasing the thickness of the films. In this study, as the thickness of the CeO_2 buffer layer increases, the tensile stresses applied to the BZT films decrease. Similar discussion in the polycrystalline $Ba_{0.50}Sr_{0.50}TiO_3$ thin films has been reported by Tenne et al. [18], who consider that the reduction of the ferroelectric transition temperature with increasing biaxial tensile stress is attributed to the suppression of in-plane polarization due to the small lateral grain size in the films ($\leqslant$100 nm). Both experimental and theoretical studies have found that even small stress can appreciably influence the Curie temperature and the dielectric permittivity and tunability of $BaTiO_3$, $SrTiO_3$, and $Ba_{1-x}Sr_xTiO_3$ (BST) thin films [19–22].

The dielectric properties of the BZT thin films in Au/BZT/Pt, and Au/BZT/CeO_2/Pt configurations are measured at room temperature as a function of the applied voltage. Fig. 4 shows the evolution of the dielectric constant and dielectric loss of the BZT thin films deposited on Pt substrates with different CeO_2 buffer layer thicknesses measured at 100 kHz. It can be seen that the dielectric constant of BZT films decreases from 249 to the